ON THE INFLUENCE OF SPIKE SHAPE
AT SUPERSONIC FLOW PAST BLUNT BODIES

UDC 533.6.07:533.69.04

Snežana S. Milićev[1], Miloš D. Pavlović[1], Slavica Ristić[2], Aleksandar Vitić[2]

[1]University of Belgrade, Faculty of Mechanical Engineering
27 marta 80, 11000 Belgrade, Yugoslavia, e-mail: milpav@alfa.mas.bg.ac.yu
[2]Technical Institute of the Yugoslav Army, Katanićeva 15, 11000 Belgrade, Yugoslavia

Abstract. *In order to eliminate the appearance of a strong shock wave at a supersonic flight of a missile, which considerably increases the drag during its flight through the air, a spike is mounted on its nose. Presented paper offers the results of an experimental analysis of the influence of the spike's shape on the aerodynamic coefficients (drag, lift and pitching moment coefficient, as well as the location of the center of pressure) at supersonic flow past blunt-nosed body. The experiment was carried out in a wind tunnel, for one value of Mach and Reynolds numbers, and for one value of the angles of attack, $\alpha = 2°$. For the body without spike, and with four different spike shapes, the aerodynamic forces and moment were measured. Using only the photos obtained by Schlieren visualization of the flow, the paper proposes a criterion of estimating the aerodynamic effect of the spike shape. The best spike shape from the experimental set of spikes, selected by the measurement of the aerodynamic coefficients, coincided with this qualitative criterion.*

Key words: *blunt-nosed body, spiked body, supersonic flow, shock wave, angle of attack, aerodynamic coefficients.*

1. INTRODUCTION

Blunt front side bodies are unpropitious for the supersonic flow, but, however, they cannot be avoided in some applications. In this case an extremely strong shock wave, as it is well known, appears in front of the body, causing an important increase of both pressure and temperature in the vicinity of the stagnation point. An intensive drag force of the body is direct result of this shock wave. Mounting a spike on the rounded nose of a blunt body moving supersonically can significantly reduce the drag force. In this way, instead of one strong shock in frontal zone, appears a system of conical waves, so that the driving force, and consequently the fuel consumption, as well as the aerodynamic heating

---

of the body, are reduced. That is why spikes are widely applied as aerodynamic constructions on supersonic planes and missiles. However, use of spike is limited due to possible appearance of oscillations, reducing the positive effects and complicating control of the body during the flight.

The fluid flow structure presented in Figure 1, based on the Wood's [1] interpretation, treats the problem of the spike's influence on the supersonic flow around the body. The characteristic fluid flow regions and discontinuity surfaces are denoted. This scheme applies to the case of a supersonic flow around a rounded nose body with a central spike, without oscillations.
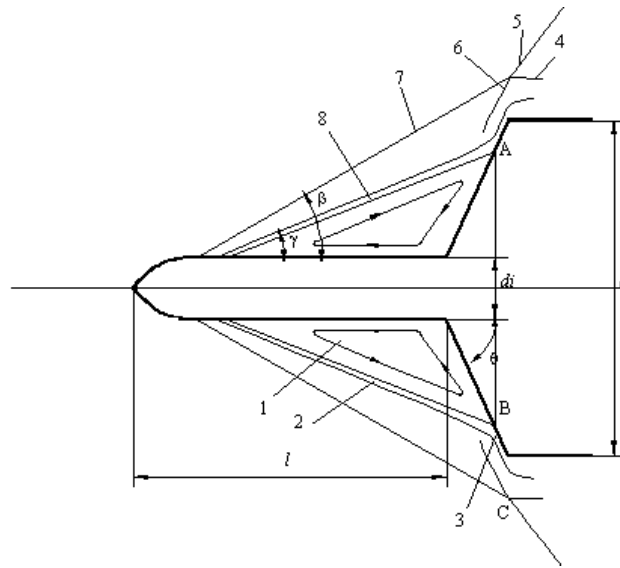

Fig. 1. Supersonic flow structure around a blunt-nosed body with spike

The recirculation zone 1 is build due to the boundary layer separation, caused by a positive pressure gradient along the spike. Outside this recirculation zone the separated boundary layer forms the zone of outer disturbed flow 2, and it reattaches to the curved surface of the body in the region 3. The outer border 8 of the recirculation zone 1 makes the cone-like surface touching the body in the plane of symmetry in the points A and B. The pressure in this region is significantly lower than behind the separated shock wave formed in front of the same body without the spike. The convective heat transfer rate from the air to the body surface is also reduced, since the velocity in this region is rather small. Only in the region of reattachment of the boundary layer, 3 occurs a great increase of the pressure and heat transfer rate from the air to the body, since the character of the flow in that region is similar to the flow around the stagnation point of the body without a spike. In the region of reattachment of the boundary layer 3 the supersonic flow declines suddenly. Due to a sudden change of flow direction the bow shock wave 6 is formed. In the point C it touches the conical wave 7, formed on the top of the spike. Since in this case the bow shock wave 6 is stronger, the greater flow-turning angle in the region 3 increases not only the drag and convective heating, but also the possibility of unwanted oscillations. This is particularly pronounced on flat front sides bodies. In this case, the

flow turning angle in the region of the reattachment of the boundary layer 3 is very large, almost 90°. The bow shock wave 6 is in this case very strong, producing the very important pressure increase behind it. This high pressure behind the shock wave 6 involves an additional air injection into the recirculation zone, provoking its enlargement, and beginning of an oscillating cycle. The oscillations can be obviously avoided by reducing the flow turning angle in the zone 3, which changes the flat front side of the body to a curved one. Due to a positive pressure gradient along the spike, as previously noted, behind the wave 7 there is a separation of the boundary layer. As a result of interaction of the waves 6 and 7 the bow wave 5 arises. Behind these three waves, starting at the point C, the shear layer 4 is formed.

During the flight of the body, there is a certain angle between the velocity vector and its axis, called the "angle of attack." Even for low values of the angle of attack, the fluid flow pattern is notably changed, but this will not be the matter of the presented paper.

Experimental investigation of the influence of the spike on the aerodynamic characteristics of blunt bodies has attracted interest of many authors. A study for bodies of revolution with flat and hemispherical noses without and with axial spikes of different lengths was given by Mair [4] in 1952, for Mach number $M_\infty = 1.96$ and for Reynolds number $Re = 1.3 \times 10^5$/cm. Bogdanoff and Vas [5] accomplished experiments looking at the influence of the spike on blunt bodies flying with hypersonic speeds for Mair [4] $12 \le M_\infty \le 14$ and for Reynolds number $Re = 0.29 \times 10^6$/cm, using two different model configurations, with flat and hemispherical noses. Their axial spike was in the form of a cylinder with a conical nose of angle 11°. The influence of the spike was studied by Hahn in [6], for $M_\infty = 3.3$ and for $Re_d = (0.12-1.91) \times 10^6$. Mair [4] and Calarese and Hankey [7] investigated the conditions for the occurrence of oscillatory flow. They accomplished their experiments on bodies with flat and hemispherical noses, concluding that for bodies with hemispherical noses, oscillatory flow does not appear.

It is evident, summarizing the cited papers, as well as excellent and detailed overviews of the most important other results given by Chang [8, 9] and Krasnov and Koshevoy [3], that different authors focused their attention predominantly on the influence of the spike's length on the aerodynamic characteristics of blunt bodies, for various angles of attack and Mach numbers. On the other side, while analyzing the fluid flow structure, presented on the Fig. 1, one might question whether the shape of the spike could affect it, and the aerodynamic characteristics of a blunt body. However, this influence has not been systematically analyzed so far. This paper tries to contribute to the study of the effect of the shape of the spike.

2. GEOMETRIC CHARACTERISTICS OF THE TESTED MODEL AND EXPERIMENTAL CONDITIONS

The geometric characteristics of the tested model are given in Fig. 2, while the four tested spike geometries are presented in Fig. 3. The model had a cylindrical body of diameter d, with the length $L = 4.44d$, with hemispherical nose, and conical tail with the semi-angle of 9°, and with the basis diameter $d_b = 0.85d$. All the four spikes were of the same length $l = d$. The Spike 1 had a cylindrical body with a conical nose with the angle of 20°. The Spikes 2 and 3 were conical with the angles of 5° and 10°. The tips of all these spikes were rounded. The Spike 4 had a hemispherical nose and a cylindrical body.

The end of each spike was conical, turning into the hemispherical nose of the model. All the four spikes, as well as the model, were made of steel and finished with high surface quality. All the components were fabricated with 1% tolerance.
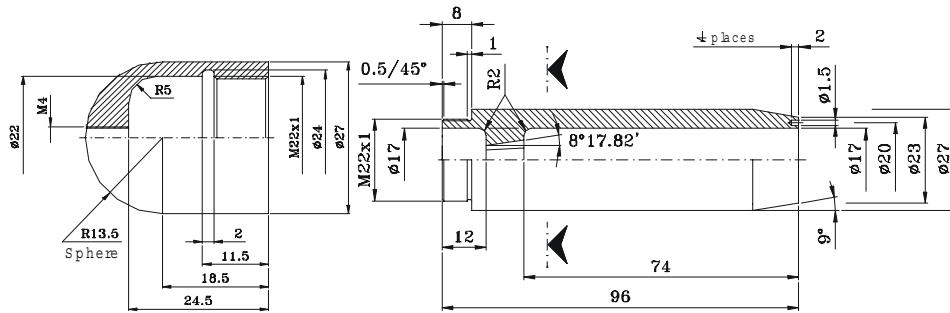

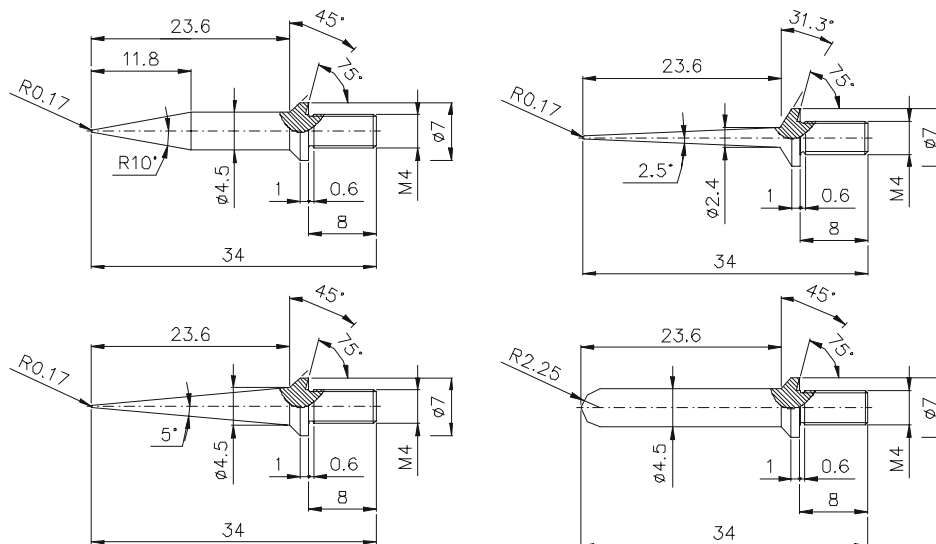Fig. 2. The tested model with hemispherical nose

Fig. 3. The four tested models of spike

The experiments were carried out in the wind tunnel T-36 in the Technical Institute of the Yugoslav Army. T-36 is a small trisonic open-wind tunnel with interrupted action. There are two vacuum reservoirs with pressure $p = 0.1$ bar and capacity $(485 + 820)$ m^3. The duration of measurement period can be up to 60s due to the reservoirs' capacity. The test tunnel has a cross section 0.25m $\times$ 0.25m and is 0.6m long. For subsonic and transonic flow, the range of Mach number can be from 0.2 to 1.1, and for supersonic flow, using different fixed nozzles, only some fixed values of Mach number can be obtained, such as $M_\infty \approx 1.56$, 1.86, 2.46, and 3.24. Reynolds number is up to 15×10^6/m for supersonic flow.

The following equipment was used during the measurements:
- Internal ROLLAB-FFA I-667 (Sweden) designed and produced strain gauge balances (six-component multipiece type), with the connection between the model and the balance made by an octagonal pyramid.
- Differential pressure transducer measuring the difference between the stagnation pressure in the silencing chamber and the static pressure in the working section of the wind tunnel, type IHTM.
- Differential pressure transducer measuring basic pressure, type PDCR42.
- Absolute pressure transducer measuring the stagnation pressure in the silencing chamber, type IHTM.
- Absolute pressure transducer measuring the pressure in the reservoir.
- Temperature sensor measuring the stagnation temperature in the silencing chamber, type RTD.
- Potentiometer in the mount of the model, measuring the angle of attack.
- Data acquisition system NEFF 600, connected to a PDP 11/84 computer for control and data treatment.
- Schlieren system for visualization of the fluid flow field. A classic Teppler system was used specially designed to meet high demands on quality and accuracy requirements.

On the basis of the measured values of stagnation pressure p_o, stagnation temperature T_o, and static pressure p, the fluid velocity v, density ρ, Mach number M_∞, and dynamic pressure q, may be estimated using the following equations:

$$M_\infty = \sqrt{[2/(\kappa-1)][(p_0/p)^{(\kappa-1)/\kappa}-1]} = \sqrt{5[(p_0/p)^{2/7}-1]}\,, \tag{1}$$

$$v = \sqrt{[2\kappa RT_0/(\kappa-1)][1-(p/p_0)^{(\kappa-1)/\kappa}]} = \sqrt{7RT_0[1-(p/p_0)^{2/7}]}\,, \tag{2}$$

$$\rho = p/RT = (p_0/RT_0)(1+M_\infty^2(\kappa-1)/2)^{-1/(\kappa-1)}\,, \tag{3}$$

$$q = pM_\infty^2\kappa/2 = pM_\infty^2\kappa/2(1+M_\infty^2(\kappa-1)/2)^{-\kappa/(\kappa-1)}\,. \tag{4}$$

Reynolds number can be obtained as:

$$\mathrm{Re}_d = vd/v = M_\infty p_0\,d/\mu\sqrt{(\kappa/RT_0)}(1+M_\infty^2(\kappa-1)/2)^{-(\kappa+1)/(2\kappa-2)}\,, \tag{5}$$

where v is the kinematics viscosity, taking the diameter of the tested model d as the characteristic length. The dynamic viscosity is calculated according to the expression:

$$\mu = 1.791\cdot 10^{-5}(T/288)^{1.5}[398.5/(110.3+T)]\,. \tag{6}$$

3. RESULTS

The experiments were performed for the model with four different types of spike, presented in the previous section, as well as for the model without spike, for supersonic flow with Mach number $M_\infty = 1.89$, and for Reynolds number $Re_d = 0.38\times10^6$. The angle of

attack α varied from −4° to 10°, with a step of 2°, but in this paper, in order to clarify the influence of the shape of spike, only its basic position, α = 2°, is taken in consideration.

During the experiments, two cycles of measurements were performed [10]. For the model without spike and for models with four different types of spike the values of the aerodynamic coefficient of drag c_d, lift c_l, pitching moment c_m, and dimensionless coordinate of the center of pressure x_{cp} were calculated and compared. The fluid flow field around the models was visualized using the Schlieren method.

3.1 Values of aerodynamic coefficients

During the experiments in the wind tunnel, using the previously quoted experimental equipment, the components of the main vector and the main moment acting on the tested models were measured, as well as all significant pressures and temperatures.

Since the velocity vector in the wind tunnel is in a vertical plane, the main force vector is also in the vertical plane, whereas the main moment is perpendicular to it. Because of that, the aerodynamic balance measures only the normal and tangential forces and the pitching moment. The aerodynamic coefficients are obtained by dividing the corresponding force or moment by the reference values of the force and moment. The dynamic pressure of undisturbed flow q is taken as the reference value of pressure, the reference area A is the cross section area of the cylindrical body of the model, while the reference length is its diameter d. The values of velocity v, density ρ, Mach number M_∞, and Reynolds number Re_d, are calculated using the expressions (1-6).

From the measured values of the normal force F_n, tangential force F_t, and pitching moment M_p, with respect to the top point of the spike, the corresponding drag coefficient c_d, lift coefficient c_l, and pitching moment coefficient c_m, are:

$$c_d = [F_n /(qA)]\sin \alpha + [F_t /(qA)]\cos \alpha , \tag{7}$$

$$c_l = [F_n / qA]\cos \alpha - [F_t / qA]\sin \alpha , \tag{8}$$

$$c_m = M_p \big/ (qAd) , \tag{9}$$

The dimensionless coordinate of the center of pressure x_{cp} is defined here as:

$$x_{cp} = (M_p / F_n - d)/l . \tag{10}$$

For each configuration, a set of experiments was undertaken, with variation of the angle of attack α. The duration of each measurement was about 20s. The measured and calculated mean values of undisturbed flow were almost the same for all the experiments:

- Silencing chamber: p_o = 0.992bar; T_o = 278K;
- Test section: p = 0.151K; T = 162K; ρ = 0.324kg/m^3; μ = 0.1097Pas;
                          q = 0.376bar; v = 482.1m/s; M_∞ = 1.89; Re_d = 0.38 ·10^6.

The influence of the four tested geometries of the spike on the aerodynamic characteristics of the blunt body is given in the Fig. 4, for the angle of attack α = 2°. When a spike is mounted on the nose of a hemispherical blunt body, regardless to its shape, a significant reduction of the drag coefficient c_d occurs, what was expected effect of such aerodynamic construction. This effect goes together with an increase of the lift

coefficient c_l, as shown in Fig. 4. It is also obvious, from the Fig. 4, that values of the pitching moment coefficient c_m are not seriously affected with the presence of the spike, except in the case of the Spike 4. The values of the dimensionless coordinate of the center of pressure x_{cp} are not seriously affected with the presence of the spike, too.
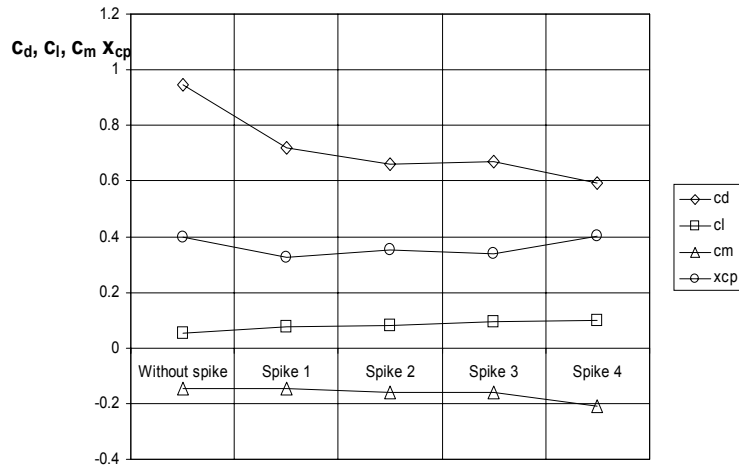

Fig. 4. The aerodynamic characteristics of the blunt body with hemispherical nose and four tested types of spike, for Mach number M=1.89 and the angle of attack $\alpha = 2^{\circ}$.

Numerical values of all aerodynamic coefficients are given in the Table 1, for the angle of attack $\alpha = 2^{\circ}$. The relative change of all aerodynamic coefficients is defined as:

$$\Delta c_{di} = c_{di} / c_d ,$$
$$\Delta c_{li} = c_{li} / c_l ,$$
$$\Delta c_{mi} = c_{mi} / c_m ,$$
$$\Delta x_{cpi} = x_{cpi} / x_{cp} .$$

(11)

where the index i denotes the type of the spike.

Table 1. The influence of the shape of the spike on aerodynamic characteristics of the blunt body with hemispherical nose for the angle of attack $\alpha = 2^{\circ}$

α [°]	c_d	Δc_{di}	c_l	Δc_{li}	c_m	Δc_{mi}	x_{cp}	Δx_{cpi}
Without spike	0.9446		0.0534		-0.147		0.3985	
Spike 1	0.6736	71.3%	0.0761	142.5%	-0.144	98.0%	0.3273	82.1%
Spike 2	0.6366	67.4%	0.0800	149.8%	-0.158	107.5%	0.3520	88.3%
Spike 3	0.6330	67.0%	0.0846	158,4%	-0.160	108.8%	0.3396	85.2%
Spike 4	0.5632	59.6%	0.0993	185.8%	-0.211	143.5%	0.4023	101.0%

The influence of the spike itself and its shape, for the presented angle of attack $\alpha = 2^{\circ}$, is notable for all types of spike, since the relative drag coefficient reduction Δc_{di} is

between 28.7% and 41.4%. It seems that the fourth spike, with a cylindrical body and a hemispherical nose, is most effective for reduction of the drag coefficient. Concerning the quantitative influence of the spike on the increase of the lift coefficient Δc_{li} it is clear that it exist for all four tested spikes. The Spike 4 gives the highest increase of the lift coefficient, 86%.

The influence of the shape of the spike on the pitching moment coefficient c_m is rather slight. For the first three spikes it is les then 10%, but for the Spike 4 it is significant, 44%. The measured value of the pitching moment coefficient is for the mass center of the body and the presented value is for the tip of a spike. The dimensionless coordinate of the center of pressure, obtained from the pitching moment coefficient and the normal force coefficient (equation 10), is presented also in the Table 1. It is obvious that mounting a spike moves the center of pressure of whole configuration towards the nose. Only for the configuration with the fourth spike the center of pressure practically does not move. For the static stability of a missile, the position of its center of pressure must be behind of the position of its mass center.

As a conclusion, the drag force for the Spike 4 has the lowest value out of all the tested cases, due to the strongest conical shock wave appearing on the tip of the spike. Thus, the pressure increase through the shock wave, appearing in front of the hemispherical nose, is smaller, as well as the total drag. This will be approved in the next subsection, by analyzing the photos obtained by the Schlieren visualization technique.

3.2 Results obtained by the Schlieren visualization technique

The visualization of the flow was carried out for a supersonic flow with Mach number $M_\infty = 1.89$, Reynolds number $Re_d = 0.38 \times 10^6$, and for the angle of attack $\alpha = 2^o$. Due to the optical adjustment of the Schlieren system used, the obtained photos, even for the angle of attack 0°, are asymmetric. No shock oscillations occurred in any direction.

In Fig 5. the Schlieren photos of the model without a spike, as well as for four tested models of spike, obtained for the angle of attack $\alpha = 2^o$ approximately, are given. For the model without spike the front of the shock wave is $a \approx 0.2d$ ahead the stagnation point. The wave attenuates alienating the body, and its angle becomes lower. This angle is reduced to approximately 45° at the distance of one diameter from the body. In the region near the shoulder of the body at the end of the hemispherical nose, behind the shock wave, an expansion wave can be noticed, with expansion lines about 55°. At the beginning of the conical tail of the body, there is also another expansion wave, with expansion lines about 44°.

For the angle of attack approximately $\alpha = 2^o$ the models with four different types of spike are presented in Fig.5. It is evident that a spike has a strong influence on the fluid flow field structure. At the tip of the spike a conical shock wave is formed accompanied with a boundary layer separation downstream. Between the wave and the spike, due to the separation, an approximately conically shaped recirculation zone is formed. There is a strong deflection of the stream in the region of the boundary layer reattachment, provoking the appearance of a curved separating shock wave. As a result of the interaction of this wave with the conical shock wave emanating from the tip, a new conical shock wave is formed. The remainder of the flow pattern is almost the same as for the body without a spike.
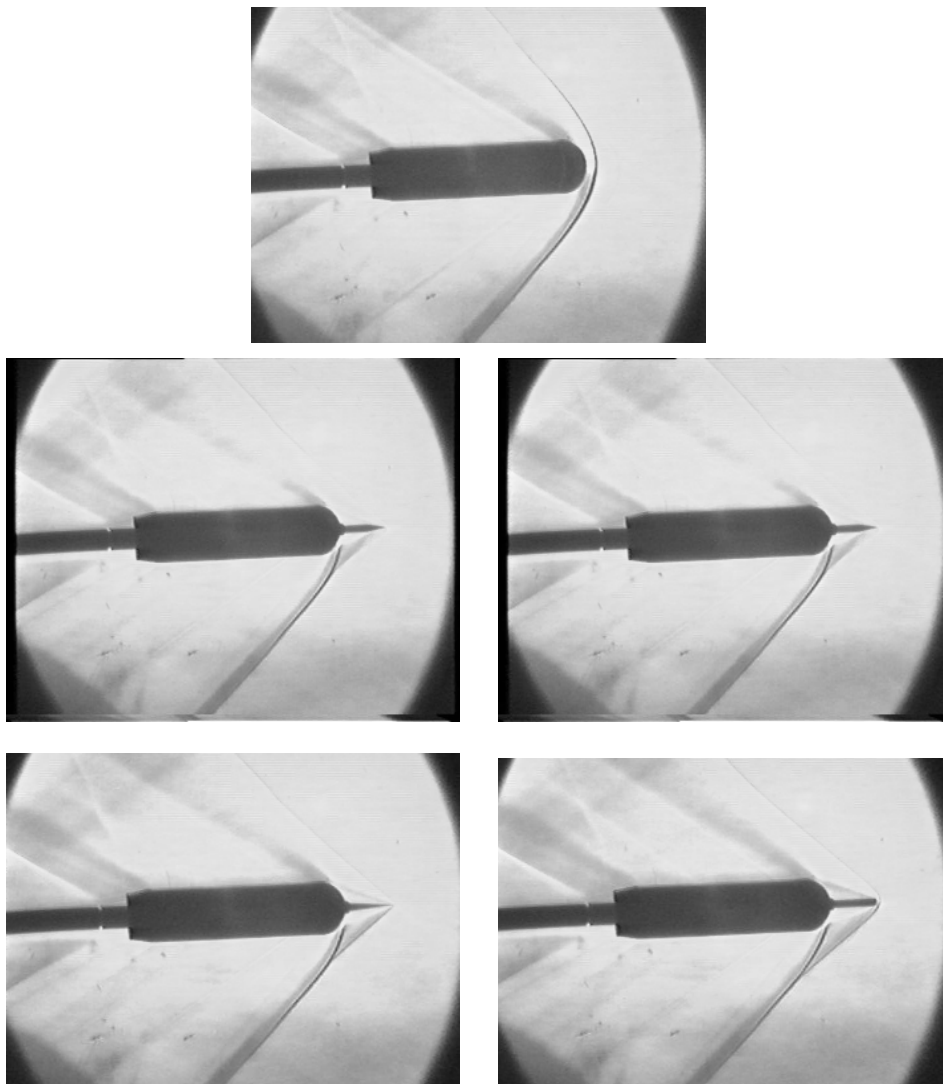
Fig. 5. Results of vizualisation by Schlieren technique for Mach number $M = 1,89$ and angle of attack $\alpha = 2^{\circ}$ for body without spike and for body with four tested models of spike.

The observed flow patterns, shown in Fig. 5, are in a good agreement with the sketch shown in Fig. 1. For various types of spike, the differences between the corresponding characteristic shock angles are of relatively minor importance. However, the principal difference that can be noted is the joint place of the leading conical shock wave, which is formed on the tip of the spike, and the separated curved shock wave, formed in the region of the boundary layer reattachment. For the Spike 1, this place is the nearest to the axis ($R_1 \approx 1.1d$), for the Spikes 2 and 3 it is $R_{2,3} \approx 1.5d$, and for the Spike 4 it is $R_4 \approx 2d$. These differences can be explained by the following reasoning. In front of the Spike 4, with a

hemispherical tip, the separated curved shock wave is stronger than the conical shock waves for the three other types with conical tips. The angle of that shock wave is $\beta \approx 45°$ when the distance from the axis varies from $0.1d$ to $0.5d$, and diminishes to the minimal value $\beta \approx 43°$ at the vicinity of its joint point with the secondary shock wave. For the Spike 1, the minimal value of that angle is $\beta \approx 39°$, and for the Spikes 2 and 3, the minimal value is $\beta \approx 42°$. The stronger shock wave at the tip of the Spike 4 is followed by the weaker second shock wave at the shoulder of the model, which is in a good agreement with the accomplished aerodynamic coefficient analysis.

Since the semi-angle of the recirculation zone is $\gamma \approx 20°$ (slightly smaller for the spike 1 and slightly bigger for the spike 4), the observed conical shock angles β correspond well to the angle of the conical shock wave which is formed in a supersonic flow ($M_\infty = 1.9$) past a cone body with the semi-angle $\gamma = 20°$ [11].

It appears that the position of the joint point of the leading and the secondary shock waves, obtained by the visualization, is a simple but reliable criterion of the aerodynamic effect of a spike. The bigger radial distance of the joint point from the axis indicates the better aerodynamic characteristics of the tested configuration.

4. VALIDATION OF THE OBTAINED RESULTS

Validation of the obtained results was possible only on the base of the lift coefficient, since they can be compared with the results of Hunt [2], with his conical tip spike. Presented results were corrected in order to reduce the base drag, for the comparison purposes. In Table 2 the results of the comparison are given, for $M_\infty = 1.89$ and for the angle of attack approximately $\alpha = 2°$. Hunt's results are denoted with the subscript *(lit)*. It seems that the agreement is quite good. The results for the models without spikes are given in the first two columns, and there is an extremely good agreement. A good agreement with Hunt's results is also obtained for the models with spikes, particularly for the Spikes 1, 2, and 3, with conical tip like his, whereas our results for the best Spike 4 are slightly higher, which could have been expected.

Table 2. Relation between the lift coefficient for the angle of attack $\alpha = 2°$ for the body: without a spike (c_{lb} - our results, $c_{lb(lit)}$ - the results of Hunt), and with the four analyzed spikes (c_{l1-4} - our results, $c_{i(lit)}$ - the results of Hunt)

α [°]	c_{lb}	$c_{lb(lit)}$	c_{l1}	c_{l2}	c_{l3}	c_{l4}	$c_{l(lit)}$
1.83	0.06	0.06	0.08	0.08	0.09	0.10	0.08

The only report found to treat the influence of geometric characteristics of a spike, to the best of our knowledge, is the paper of Daniels and Yoshihara [12]. Two types of spike, with flat and conical tips, and with length $l > 1.5d$, for higher values of Mach number were analyzed, so that a quantitative comparison is not possible here. However, their conclusions that the spike with a flat tip, provoking a stronger leading shock wave appearing in front of the tip, is better than the spike with a conical tip, can be taken as a qualitative verification of our results.

5. CONCLUSION

The influence of different shapes of a spike mounted on a hemispherical nose of a symmetric body, in a supersonic flow has been treated experimentally in the presented paper. Four different spikes, with different tips, of the length equal to the body diameter. The experiments were performed in a small trisonic wind tunnel, with Mach number $M_\infty = 1.89$ and Reynolds number $Re_d = 0.38 \times 10^6$. The angle of attack was $\alpha = 2^o$. In order to obtain the lift coefficient, the drag coefficient, and the pitching moment coefficient, the measurements of the aerodynamic load of the model were carried out. It has been shown that the shape of the spike has an important influence on the aerodynamic characteristics of the model. The Spike 4, with a cylindrical body and a rounded tip, has been found to have the best aerodynamic characteristics. For this type of spike the drag coefficient c_d is significantly reduced (~40%), and the lift coefficient c_l is notably raised (~85%), in comparison with the same model without a spike. Value of the pitching moment coefficient c_m is also higher (~44%), but the position of the centre of pressure x_{cp}, is practically the same in comparison with the same model without spike.

Visualization experiments were performed in the same wind tunnel, using the Schlieren technique, in order to explain the obtained results for aerodynamic coefficients. In the case of the spike with a rounded tip (Spike 4), the leading shock wave appearing at the tip is curved, separated, and stronger than the conical shock wave appearing at a sharpen tip in the case of the other tested geometries (Spikes 1, 2 and 3). However, this implies that the following, second shock wave, appearing at the shoulder of the body, is stronger for the leading conical shock wave. The total loss of mechanical energy is therefore less for the curved and separated leading shock wave. This explains the better aerodynamic coefficients for the best Spike 4.

This reasoning has lead to a formulation of a simple yet reliable criterion for estimating aerodynamic effects of a spike by using visualization only. The bigger the radial distance of the joint point of the leading and the secondary shock waves from the axis, the better aerodynamic characteristics of the tested configuration.

REFERENCES

1. Wood, C. J., *A Study of Hypersonic Separated Flow*, Ph. D. thesis, University of London, October 1961 (available as DDC Ad 401652)
2. Hunt, G. K., *Supersonic Wind Tunnel Study of Reducing the Drag of a Bluff Body at Incidence by Means of a Spike*, Royal Aircraft Establishment, Rept. Aero 2606, May 1958
3. Krasnov, N. F., Koshevoy, V. N., *Control and stabilization in aerodynamics* (in Russian), High school, Moscow, 1978
4. Mair, W. A., *Experiments on Separation of Boundary Layers on Probes in Front of Blunt-Nosed Bodies in a Supersonic Air Stream*, Phil. Mag., Ser. 7, Vol. 43, No. 342, July 1952, pp. 695-716
5. Bogdonoff, S. M., Vas, I. E., *Preliminary Investigations of Spiked Bodies at Hypersonic Speeds*, J. Aero/Space Sciences, Vol. 26, No. 2, February 1959, pp. 65-74
6. Hahn, M., *Pressure Distribution and Mass Injection effects in the Transitional Separated Flow over a Spiked Body at Supersonic speed*, J. Fluid Mech., Vol. 24, Part 2, 1966, pp. 209-223
7. Calarese, W., Hankey, W. L., *Modes of Shock-Wave Oscillations on Spike-Tipped Bodies*, AIAA Journal, Vol. 23, No. 2, February 1985, pp. 185-192

8. Chang, P. K., *Ames Research Staff*, Hemisphere Publishing Corporation, 1976
9. Chang, P. K., *Separation of Flow*, Pergamon Press, 1970
10. Milićev, S., *Supersonic Flow around Blunt Bodies of Revolution with Spike*, (in Serbian), M. Sc. Thesis, University of Belgrade, Faculty of Mechanical Engineering, Belgrade, 1999
11. Ames Research Staff, *Equations, Tables, and Charts for Compressible Flow*, National Advisory Committee for Aeronautics, Report 1135
12. Daniels, L.E., Yoshihara, H., *Effects of the Upstream Influences of a Shock Wave at Supersonic Speeds in the Presence of a Separated Boundary Layer*, WADC Tech. Rept. 54-31, January 1954

O UTICAJU IGLE NA NADZVUČNO STRUJANJE OKO ZAOBLJENOG TELA

Snežana S. Milićev, Miloš D. Pavlović, Slavica Ristić, Aleksandar Vitić

Da bi se eliminsala pojava jakog udarnog talasa pri nadzvučnom opstrujavanju projektila, koja zanačajno povećava otpor pri letu krozvazduh, na njegov vrh montira se igla. U radu se daju rezultati eksperimentalnog istraživanja uticaja oblika igle na aerodinamičke koeficijente (uzgona, otpora, momenta propinjanja, kao i položaj centra pritiska) pri nadzvučnom opstrujavanju tela zaobljenog vrha. Eksperiment je izveden u aereotunelu, za jednu vrednost Mahovog i Rejnoldsovog broja, kao i za jednu vrednost napadnog ugla α = 2º. Za telo bez igle, kao i za telo sa četiri različita modela igle merene su aerodinamičke sile i momenti. U radu su predloženi kriterijumi za procenu uticaja igle zasnovani isključivo na rezultataima dobijrenim vizualizacijom strujanja. Igla najboljih karakteristika, od ispitanih konfiguracija, izabrana na osnovu izmerenih aerodinamičkih koeficijenata, uklapa se u ove kvalitativne kriterijume.